Kelvin Wave Packets and Flow Acceleration: A Comparison of Modeling and Observations[1]

LAWRENCE COY[2] AND MATTHEW HITCHMAN

Department of Atmospheric Sciences, University of Washington, Seattle, WA 98195

(Manuscript received 3 October 1983, in final form 6 February 1984)

ABSTRACT

Atmospheric Kelvin waves, as revealed by temperatures obtained from the recent Limb Infrared Monitor of the Stratosphere (LIMS) experiment, commonly occur in packets. A simple two-dimensional gravity-wave model is used to study the upward propagation of these packets through different zonal mean wind profiles derived from the LIMS data. The observed prevalence of high frequency waves in the lower mesosphere and low frequency waves in the lower stratosphere can be explained by dispersion of energy associated with the range of frequencies comprising a packet. Dominant wave frequencies at upper and lower levels are more distinctly separated if the packet propagates through a layer of westerly winds. Due to dispersion and shear effects, a packet of short temporal length at low levels will have a considerably extended impact on a layer of westerly winds at higher levels. Observed and modeled westerly accelerations resulting from packet absorption occur in the same layer, and are similar in magnitude and duration. These results support the theory that Kelvin waves are responsible for the westerly phase of the semiannual oscillation.

1. Introduction

One of the most thought-provoking aspects of equatorial dynamics has been the discovery of recurring, long-lasting layers of zonal mean westerlies in the altitude range 16–90 km. Zonal mean winds at extratropical latitudes are never observed to have greater angular momentum than the earth's equator. Thus equatorward motion can only generate easterlies over the equator. The existence of these westerlies is now believed to be due to the vertical redistribution of momentum by zonally asymmetric equatorial Kelvin waves. In the altitude range ~ 16–40 km, successive westerly and easterly regimes are observed to form at upper levels and descend with time in the phenomenon known as the quasi-biennial oscillation (QBO). At the solstices, westerlies are observed to form near the mesopause (~90 km) and descend at a rate of ~10 km per month to the middle stratosphere (~30 km), being replaced twice yearly by easterlies in the more periodic phenomenon known as the semiannual oscillation (SAO). The structure of the Kelvin wave, the QBO and the SAO in the vicinity of the stratopause, and the Kelvin-wave forcing mechanism, are reviewed by Wallace (1973) and Holton (1975).

Kelvin waves of period $\tau \sim 15$ days and vertical wavelength $L \sim 6$–10 km have been detected in tropical rawinsonde data in the altitude range 16–30 km. They are more prevalent in easterlies and are believed to explain the formation and descent of QBO westerlies. Using Ascension Island rocketsonde data, Hirota (1978) presented evidence for 15–20 km wavelength Kelvin waves in the altitude range 25–60 km. He found the waves to be more active during times of SAO easterlies and when QBO easterlies prevailed in the lower stratosphere. Using data from a nadir-viewing satellite, Hirota (1979) was able to show evidence for 4–10 day Kelvin waves in the same altitude range. These observations have provided somewhat limited descriptions of Kelvin waves: station profiles sample only limited regions, while nadir-viewing, polar-orbiting satellites sample the globe, but with poor vertical resolution. They suggest, however, that short, low frequency Kelvin waves are involved in the QBO and that taller, higher frequency Kelvin waves are involved in the SAO below 60 km.

The existence of the SAO in the layer 60–90 km was detected in rocketsonde data taken at Ascension Island (Hirota, 1978) and at Kwajalein (Hamilton, 1982). The data show that the SAO amplitude maximizes at the mesopause and stratopause, that it is exactly out of phase at these two levels, and that time-mean westerlies exist between. Indeed, Dunkerton (1982) suggests that SAO easterlies at the two maximum levels have separate driving mechanisms. However, downward propagation of westerlies is continuous from 90 to 30 km; Kelvin waves are again likely to be responsible for mesopheric westerlies.

Evidence that Kelvin waves exist at levels above 60

[1] Contribution No. 674, Department of Atmospheric Sciences, University of Washington, Seattle.

[2] Present affiliation: NOAA/ERL, Boulder, CO 80303.

km has come from the recent Limb Infrared Monitor of the Stratosphere (LIMS) experiment. With the combined advantages of global data coverage and high vertical resolution, the LIMS instrument has provided a uniquely detailed picture of the temperature structure in the equatorial middle atmosphere (Gille and Russell, 1984). Salby *et al.* (1984) present spectrally analyzed data which reveal Kelvin zonal waves one and two to each have power peaks at periods near 4 and 7 days, with the higher frequency waves appearing mainly in the lower mesosphere. Hayashi *et al.* (1984) have recently detected Kelvin waves of periods ~ 15, 7 and 4 days in the lower stratosphere, upper stratosphere and mesosphere, respectively, by spectral analysis of disturbances in a general circulation model.

Here we use daily values of temperature, rather than values which have been band-passed in frequency, to illustrate that Kelvin waves often propagate as wave packets. The gravity-wave model is then used to study Kelvin wave packet propagation through two different mean wind profiles taken from the LIMS data. We attempt to show that separation of dominant frequencies with altitude may be due to packet dispersion and selective absorption in shear. Mean flow changes produced by model wave packets are then compared with observed changes.

2. Observations

The data used here are daily synoptic values of LIMS temperature at 1200 GMT on 25 October 1978–28 May 1979. Thirteen zonal harmonic coefficients are available at 4° intervals from 64°S to 84°N and at 18 standard levels between 100 and 0.05 mb (~16–70 km). Leovy *et al.* (1984) show that equatorial zonal wind profiles derived from LIMS temperatures, exhibiting regions of strong vertical shear, agree remarkably well with rocketsonde profiles of zonal wind. They present a time–height section of the equatorial SAO in zonal wind for the 216-day data record.

The two wind profiles in Fig. 1 were selected from the LIMS data as being representative of two different phases of the SAO. The dashed curve corresponds to mid-November 1978, when a layer of SAO westerlies was centered near 40 km. The solid curve corresponds to late January 1979, when the next westerly wind layer (visible above 64 km in the dashed curve) has filled out the lower mesosphere. Easterlies existed throughout the region 24–51 km in January. QBO westerlies are present below 24 km in both curves. The presence of westerlies at the lowest levels may help explain the near absence of the 15-day Kelvin wave in the LIMS data.

Figures 2a and b show time–height sections of zonal-wave-two amplitude at 0° longitude for the periods 25 October–7 December 1978 and 15 January–17 February 1979. Equatorial time–height sections of LIMS wave temperatures exhibit considerable detail.

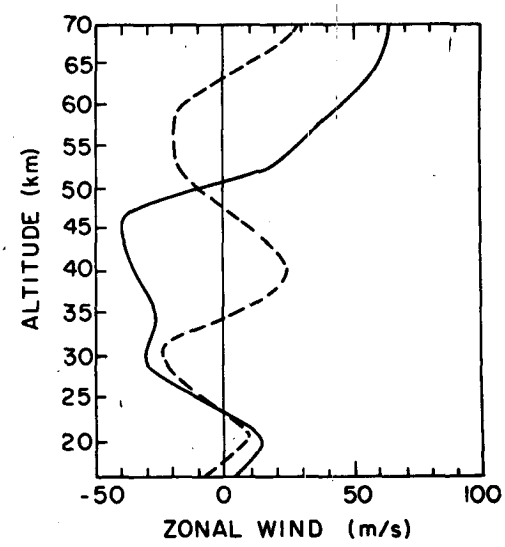

FIG. 1. LIMS zonal mean wind profiles at the equator corresponding to mid-November 1978 (dashed curve) and late January 1979 (solid curve).

With a nominal vertical field of view at the limb of 1.8 km, vertical wavelengths larger than ~6 km are resolved. Random errors are smaller than 1 K, but systematic errors can be ~2–3 K at levels below 1 mb (Gille *et al.*, 1984). Thus, the features of interest are those which exhibit good coherence in time and space and behave according to theoretical expectations. LIMS wave temperatures have been examined in detail in daily sequences of other projections (not shown). Most of the perturbations seen in Figs. 2a and b may be classified, according to behavior, as manifestations of Kelvin waves, Rossby waves of midlatitude origin, or inertial waves (which have only recently been predicted by theory). In all LIMS sections in this paper, values contoured are the average of those at 8°S, 4°S, 0°, 4°N and 8°N. Such an average emphasizes the Kelvin wave, which is known to be symmetric about the equator. The straight lines indicate regions where groups of vertically propagating Kelvin waves are present.

Since the horizontal wavelength is much larger than the vertical wavelength, Kelvin-wave vertical motions are essentially hydrostatic. The dispersion relation for such a gravity wave is

$$\omega - \bar{u}k = -Nk/\lambda \qquad (1)$$

(Holton, 1979), where ω is the frequency, k the zonal wavenumber, λ the vertical wavenumber, $\bar{u}$ the zonal average of the zonal wind, and N the buoyancy frequency. For $\omega > \bar{u}k$ and $\lambda < 0$, there is eastward and downward phase propagation and upward energy propagation. The vertical group velocity $G \equiv \partial\omega/\partial\lambda$ is

$$G = Nk/\lambda^2 = (\omega - \bar{u}k)^2/Nk. \qquad (2)$$

Week-to-week variations in the intensity of equa-

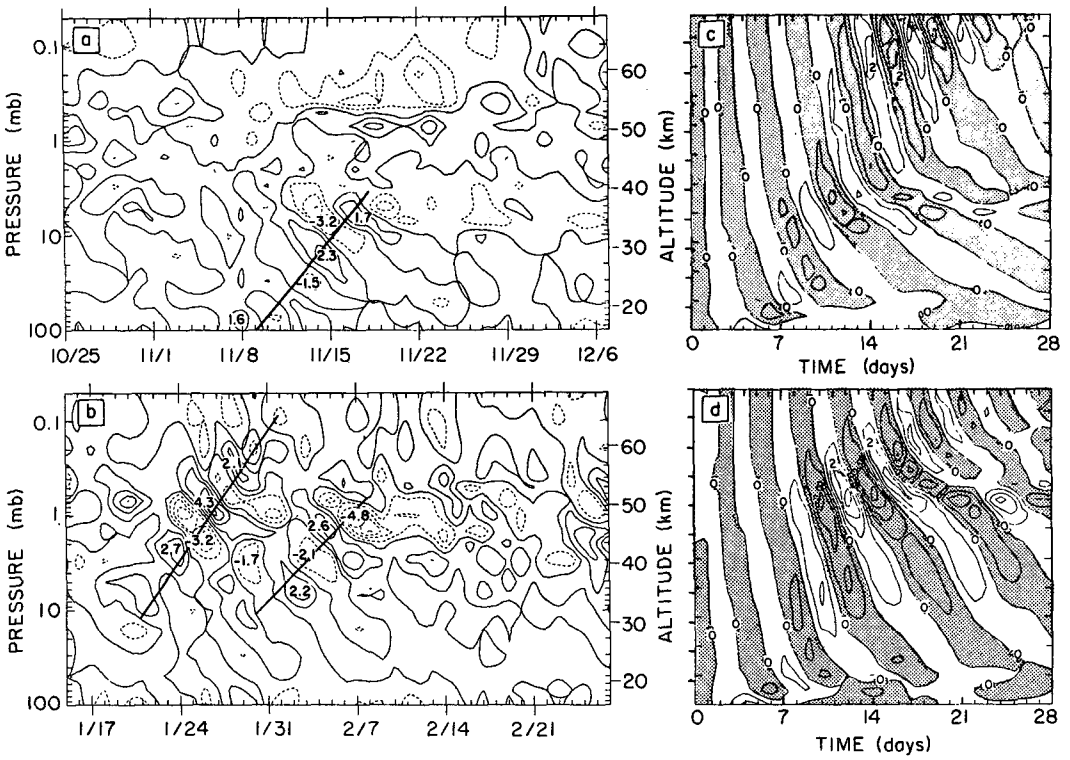

FIG. 2. Equatorial time–height sections of LIMS zonal wave 2 temperature at 0° longitude for the periods (a) 25 October–7 December 1978 and (b) 15 January–27 February 1979, and of model wave 2 temperature at fixed longitude for runs using (c) the dashed initial mean wind profile of Fig. 1 and (d) the solid profile. Contour interval is 1 K.

torial tropospheric phenomena are likely to be responsible for the frequently observed packet nature of Kelvin waves. Variations in forcing necessarily excite a range of frequencies. Eq. (2) shows that, for a given zonal wind, energy associated with different frequencies travels at different rates and the waves disperse. Thus, high frequency waves readily penetrate a layer in which low frequency waves approach a critical level ($\omega - \bar{u}k \rightarrow 0$). These low frequency waves will be absorbed by damping processes as their wave energy remains in the layer. Amplitude decreases with height are indicative of wave absorption which, for the eastward-moving Kelvin wave, implies an eastward acceleration of the mean flow.

In Fig. 2a, a group, or energy envelope, appears to originate at the tropopause in the period 5–12 November and ascend at a rate of ~2.8 km day^{-1} to near 40 km, above which it is not observed to propagate. The packet appears to be absorbed near this level, where there is a westerly wind maximum of 28 m s^{-1}. Individual waves are seen to form on the leading edge of the packet and propagate downward at about the same rate. Near 15 November and 30 km, $\tau \sim 6$ days and $L \sim 15$ km. There is a tendency for waves to the upper left of the straight line to be taller and of a higher frequency, and for waves to the lower right to be shorter and of lower frequency. However, using these modal values of τ and L in (2), the lines of constant phase should move downward at the rate $\omega/\lambda \sim -2.5$ km day^{-1} and the vertical group velocity (taking $N = 0.02$ s^{-1} and $k = 2/6.4 \times 10^6$ m^{-1}) should be 3.1 km day^{-1}. The wave motions are explained fairly well by simple gravity-wave theory.

The situation in Fig. 2b is more complex. Two packets appear to propagate readily through easterlies until the westerlies are reached near 55 km. Individual waves above this level have distinctly higher frequencies and larger vertical wavelengths than those below. Near 65 km and 28 January, $L \sim 20$ km and $\tau \sim 3.5$ days, hence this wave has a zonal phase speed of ~65 m s^{-1}. It is this type of wave which is likely to reach the mesopause and instigate the next SAO westerly layer.

3. Numerical model

To investigate the vertical propagation of Kelvin wave packets, a two-dimensional, hydrostatic, internal gravity wave model was integrated using typical Kelvin wave parameters. The model (Coy, 1983) is similar to other two-dimensional gravity-wave models (e.g., Jones and Houghton, 1971; Breeding, 1972). The equations describing a two-dimensional gravity wave are the zonal momentum, thermodynamic energy, continuity and hydrostatic equations. A semi-implicit time-differencing scheme leads to a single equation for the vertical structure of perturbation geopotential height at the

new time. This vertical structure equation is then solved by using a tri-diagonal algorithm, as in atmospheric tidal theory (Chapman and Lindzen, 1970). The new velocity field can then be calculated from the new height field. The model is "quasi-linear" in that the wave stress is allowed to change the mean flow, and mean flow changes affect wave propagation, but only a single zonal harmonic is considered so that wave–wave interactions are neglected. Both the scale height H and the buoyancy frequency N are assumed to be independent of height and are taken to be 7 km and 0.02 s^{-1}, respectively. The vertical model domain is 16–91 km. A rigid lid is used as the upper boundary condition. Reflections from the upper boundary are prevented by including a large damping above 70 km.

Kelvin waves in the middle atmosphere have periods longer than one day, are trapped at low latitudes, and do not propagate meridionally. Wave amplitudes decrease exponentially away from the equator, with quarter-power distances being ~15° latitude (Salby *et al.*, 1984). Rotation is neglected in the present model. We have seen that, to a large extent, the Kelvin wave resembles a two-dimensional gravity wave propagating in longitude and altitude. However, the size of the energy envelope in latitude is known to depend on the zonal mean wind. Thus, accurate wave amplitudes and momentum fluxes may not be realizable in this model, where meridional structure of the Kelvin waves and zonal mean meridional circulations are ignored. In particular, magnitudes of calculated changes in zonal mean wind should be interpreted with some caution (see Plumb and Bell, 1982). However, the present model is in the spirit of the Kelvin wave models considered by Plumb (1977) and Dunkerton (1981). Here we concentrate on the effects of forcing variations in time.

Waves in the model are forced at the lower boundary by specifying the temperature perturbation as

$$T = AF(t)\sin(Kx - \Omega t), \tag{3}$$

where $A = 1.73$ K, $\Omega = 1.1 \times 10^{-5}$ s^{-1}, $K = 2/6.4 \times 10^{6}$ m^{-1}, and the packet is due to the modulation

$$F(t) = \begin{cases} \sin^2\left(\frac{\pi}{2}\frac{t}{4\text{ days}}\right), & 0 \leq t \leq 8\text{ days} \\ 0, & t > 8\text{ days.} \end{cases} \tag{4}$$

The modal wave will have a zonal phase speed Ω/K, or 35 m s^{-1}.

First the model was run linearly (no mean flow changes) with no initial mean wind and no damping, except for the sponge layer above 70 km. The duration of forcing (8 days) is close to the modal period (6.6 days) so that dispersive effects should be important. The results for this run (Fig. 3) show that the wave envelope spreads out as it goes up. High frequency components appear at upper levels while low frequency components remain at lower levels.

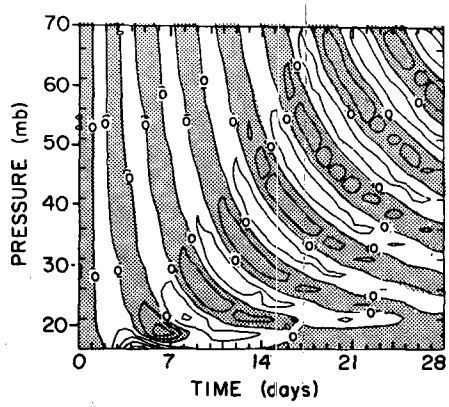

FIG. 3. Time-height section of model zonal wave 2 temperature at a fixed longitude for a run with a nonvarying zero initial mean wind profile. The results are scaled by $\exp(z/2H)$ and the contour interval is 1 K.

Figures 2c and d are results of model runs using the dashed and solid curve initial mean wind profiles of Fig. 1. To offset the exponential growth with height of wave amplitudes due to decreasing density, a Newtonian temperature perturbation damping coefficient, zero below 27 km, and increasing linearly from zero at 27 km to 1 per day at 70 km, was included. Mean wind variations with height distort the dispersion pattern of Fig. 3. As in the observations, there is a marked frequency separation above and below the mean wind peak of 28 m s^{-1} at 40 km in the November case and the critical level (for the modal wave) at 57 km in the January case.

Another strong similarity with the observations is the tendency for some of the wave activity to linger in westerly shear below the mean wind maximum in the two cases. However, observed packet absorption appears to be stronger than in the model for the November case. Model damping may be too weak. Perhaps the forcing should be longer than 8 days. This would increase the amplitude of the 35 m s^{-1} wave relative to slower and faster waves. A third possibility is that the curious layered disturbance present above 45 km is obscuring or disrupting Kelvin wave propagation. These long-lasting, non-propagating temperature perturbations occur during periods of strong cross-equatorial shear. They are believed to indicate the presence of low-wavenumber circulation cells in the latitude–height plane, correspond well with inertial instability theory, and will be the subject of a future paper.

In the January case, modeled and observed dispersion patterns near 50 km are remarkably similar. What appears to be two packets in the observations may actually be the result of one forcing event. The model results also show that if a 35 m s^{-1} wave is forced for a sufficiently short time, enough amplitude will exist at higher frequencies to account for the observed 65 m s^{-1} wave in the lower mesosphere.

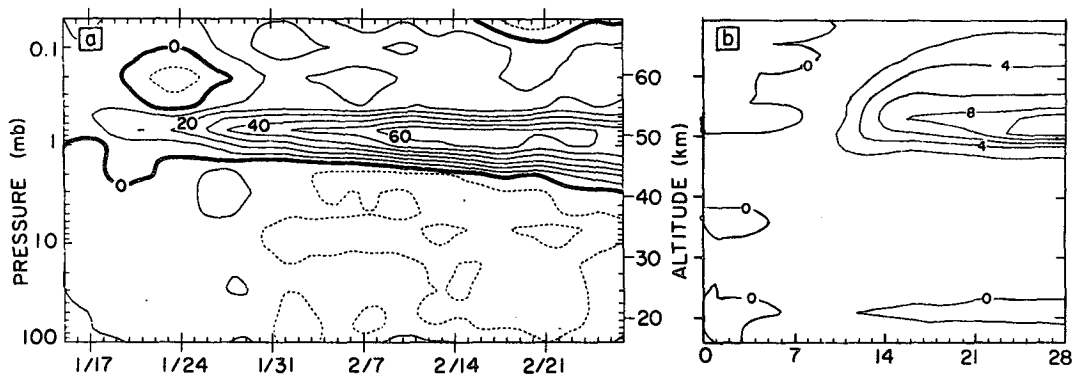

FIG. 4. Time–height sections of (a) observed and (b) modeled changes in zonal mean wind $u - \bar{u}_0$ for the January case. In (a), $\bar{u}_0$ is the LIMS profile for 15 January 1979 and the contour interval is 10 m s^{-1}. In (b), $\bar{u}_0$ is the solid curve initial mean wind profile in Fig. 1 and the contour interval is 2 m s^{-1}.

Figure 4 shows the time change in zonal mean wind as observed and modeled for the January case. The LIMS data have been smoothed with a 1–2–1 filter in time to reduce day-to-day noise. The model wave packet accelerates the mean flow near 50 km for over two weeks (Fig. 4b), although the wave forcing lasts only 8 days (Fig. 2d). Observed wave activity (Fig. 2b) and accelerations (Fig. 4a) are strongest at the base of the descending SAO westerly layer during 24 January–9 February.

During this time at 50 km, observed flow acceleration averages 2.5 m s^{-1} day^{-1}, although the largest model accelerations are only $\sim$1 m s^{-1} day^{-1}. In the real atmosphere wave-one packets would also be expected to contribute to this large observed acceleration. In the LIMS data, zonal-wave-one packets (not shown) are incident on the westerlies near 50 km at much the same time as the wave-two packets, but with temperature amplitudes about twice as large. Downward advection of westerlies by Kelvin-wave induced mean meridional circulations may also contribute significantly to the observed westerly acceleration.

Wave dispersion and trapping near critical levels ensure that a packet of rather short duration near its forcing level has a protracted effect on the mean flow. In both the model results and observations, the tendency for wave activity to linger in the westerly shear is associated with further acceleration at levels below 50 km. These results support the hypothesis that irregular forcing of Kelvin wave packets near the equatorial tropopause can result in the observed smooth descent of SAO westerlies.

4. Conclusions

The LIMS data show that Kelvin waves in the region of the SAO vary in amplitude. These variations can be described as wave packets propagating with the vertical group velocity given by linear wave theory. The separation into progressively higher dominant frequencies found to be associated with the QBO, the stratopause SAO and the mesopause SAO can be explained in terms of packet dispersion and selective absorption. Modeling results show that the mean flow changes produced by the waves can account for the westerly winds of the SAO. A more quantitative study using observed wave amplitudes to calculate expected accelerations for the whole data record is currently being pursued. The modeling studies could be improved by developing more realistic radiative damping and including a tropospheric source region. Any complete simulation should also consider the meridional variations of both the waves and mean flow.

Acknowledgments. We wish to thank Professor Conway Leovy for many useful discussions and Nancy Wytko for typing the manuscript. This work was supported by NASA Grants NA2-66, NASI-14341 and NAGW-471.

REFERENCES

Breeding, R. J., 1972: A nonlinear model of the breakup of internal gravity waves due to their exponential growth with height. *J. Geophys. Res.*, **77**, 2681–2692.

Chapman, S., and R. S. Lindzen, 1970: *Atmospheric Tides.* D. Reidel, 200 pp.

Coy, L., 1983: The vertical propagation of internal gravity waves in a compressible atmosphere. Ph.D. dissertation, University of Washington, 195 pp.

Dunkerton, T. J., 1981: Wave transience in a compressible atmosphere. Part II: Transient equatorial waves in the quasi-biennial oscillation. *J. Atmos. Sci.*, **38**, 298–307.

——, 1982: Theory of the mesopause semiannual oscillation. *J. Atmos. Sci.*, **39**, 2681–2690.

Gille, J. C., and J. M. Russell, III. 1984: The Limb Infrared Monitor of the Stratosphere (LIMS) Experiment description, performance and results. *J. Geophys. Res.*, **89** (in press).

——, ——, P. L. Bailey, L. L. Gordley, E. E. Remsberg, J. H. Lienesch, W. G. Planet, F. B. House, L. V. Lyjak and S. A. Beck, 1984: Validation of temperature retrievals obtained by the Limb Infrared Monitor of the Stratosphere (LIMS) experiment on Nimbus 7. *J. Geophys. Res.*, **89** (in press).

Hamilton, K., 1982: Rocketsonde observations of the mesospheric

semiannual oscillation of Kwajalein. *Atmos. Ocean,* **20,** 281–286.

Hayashi, Y., D. G. Golder and J. D. Mahlman, 1984: Stratospheric and mesospheric Kelvin waves simulated by the GFDL "SKYHI" general circulation model. *J. Atmos. Sci.,* **41,** 1971–1984.

Hirota, I., 1978: Equatorial waves in the upper stratosphere and mesosphere in relation to the semiannual oscillation of the zonal wind. *J. Atmos. Sci.,* **35,** 711–714.

——, 1979: Kelvin waves in the equatorial middle atmosphere observed by the Nimbus 5 SCR. *J. Atmos. Sci.,* **36,** 217–222.

Holton, J. R., 1975: *The Dynamic Meteorology of the Stratosphere and Mesosphere. Meteor. Monogr.,* No. 37, Amer. Meteor. Soc., 216 pp.

——, 1979: *An Introduction to Dynamic Meteorology.* 2nd ed., Academic Press, 381 pp.

Jones, W. L., and D. D. Houghton, 1971: The coupling of momentum between internal gravity waves and the mean flow: A numerical study. *J. Atmos. Sci.,* **28,** 604–608.

Leovy, C. B., M. H. Hitchman, A. K. Smith, J. C. Gille, P. L. Bailey, E. E. Remsberg and M. L. Salby, 1984: Properties of quasi-global fields of temperature, geopotential, and wind derived from the Nimbus 7 LIMS experiment. *J. Geophys. Res.,* (In preparation).

Plumb, R. A., 1977: The interaction of two internal waves with the mean flow: Implications for the theory of the quasi-biennial oscillation. *J. Atmos. Sci.,* **34,** 1847–1858.

——, and R. C. Bell, 1982: A model of the quasi-biennial oscillation on an equatorial beta-plane. *Quart. J. Roy. Meteor. Soc.,* **108,** 335–352.

Salby, M. L., D. L. Hartmann, P. L. Bailey and J. C. Gille, 1984: Evidence for equatorial Kelvin modes in Nimbus-7 LIMS. *J. Atmos. Sci.,* **40,** 220–235.

Wallace, J. M., 1973: General circulation of the tropical lower stratosphere. *Rev. Geophys. Space Phys.,* **11,** 191–222.